Diabetes, Metabolic Syndrome and Obesity

Dovepress
Taylor & Francis Group

Open Access Full Text Article

ORIGINAL RESEARCH

PEDF Overexpression Ameliorates Cardiac Lipotoxicity in Diabetic Cardiomyopathy via Regulation of Energy Metabolism

Tuohua Mao, Ye Wang

Department of Endocrinology, Renmin Hospital of Wuhan University, Wuhan, 430060, People's Republic of China

Correspondence: Ye Wang, Department of Endocrinology, Renmin Hospital of Wuhan University, 238 Jiefang Road, Wuchang, Wuhan, Hubei, 430060, People's Republic of China, Email wye2018@whu.edu.cn

Background: Early alterations in cardiac energy metabolism and lipotoxicity are crucial factors in the pathogenesis and progression of diabetic cardiomyopathy (DCM). The excessive accumulation of lipid metabolic intermediates within the myocardium can lead to increased production of reactive oxygen species (ROS) and promote apoptosis. Pigment epithelium-derived factor (PEDF) has been shown to regulate cardiac energy metabolism; however, its role in modulating energy metabolism, ROS generation, and apoptosis in the context of DCM requires further investigation.

Methods: PEDF was overexpressed in db/db mice via tail vein injection of adeno-associated virus 9(AAV9)-PEDF. At week 24, assessments were conducted on cardiac hypertrophy, fibrosis, cardiac function, and alterations in energy metabolism. Additionally, H9c2 cells were transfected with a PEDF plasmid and cultured under HG+PA conditions (33 mm glucose + 250 μM palmitic acid) for 24 hours. Subsequent analyses focused on changes in energy metabolism, ROS levels, and apoptosis.

Results: At 24 weeks, db/db mice exhibited hallmark features of DCM, including hyperglycemia, hyperlipidemia, cardiac hypertrophy, fibrosis, and diastolic dysfunction. Overexpression of PEDF reversed cardiac remodeling in these mice. In both db/db mice and HG+PA-treated H9c2 cells, PEDF overexpression modulated cardiac energy metabolism, mitigated lipotoxicity, and promoted the expression of adipose triglyceride lipase(ATGL) and glucose transporter type 4(Glut4) while inhibiting the expression of peroxisome proliferator-activated receptor alpha (PPARα), carnitine palmitoyltransferase 1 alpha (CPT1α), and scavenger receptor B2 (CD36). Additionally, PEDF overexpression reduced ROS generation and apoptosis in db/db mice myocardium and HG+PA-treated h9c2 cells.

Conclusion: PEDF can effectively prevent cardiac hypertrophy, fibrosis remodeling, and the deterioration of diastolic dysfunction in DCM by modulating cardiac energy metabolism and mitigating ROS production and apoptosis induced by lipotoxicity.

Keywords: PEDF, diabetic cardiomyopathy, metabolic disorders, lipotoxicity, reactive oxygen species, apoptosis

Introduction

With the increasing prevalence of diabetes year by year, diabetic complications pose a threat to the quality of life for patients and impose a significant economic burden worldwide. Previous studies have indicated that approximately 50–80% of individuals with diabetes succumb to cardiovascular complications, and diabetics face a 2 to 4 times higher risk of heart failure compared to those without diabetes.[1] Diabetic cardiomyopathy (DCM), resulting from diabetes in the absence of hypertension and coronary artery disease, is characterized by profound structural remodeling and progressive deterioration of cardiac function, ultimately culminating in heart failure and mortality.[2] The pathogenesis of DCM remains elusive. Studies have demonstrated that insulin resistance, myocardial lipotoxicity, myocardial glucotoxicity, apoptosis, oxidative stress, mitochondrial dysfunction, and autophagy play pivotal roles in the development of DCM.[3–6] In the past few decades, significant advancements have been made in both basic and clinical research on DCM. However, there is still a lack of effective strategies for preventing or ameliorating DCM in diabetic patients. Therefore, it is imperative to delve into the molecular mechanisms underlying the onset and progression of DCM.

Received: 12 June 2024
Accepted: 22 January 2025
Published: 27 January 2025

The pathogenesis of diabetic cardiomyopathy is multifaceted; however, the initial alterations in cardiac energy metabolism play a pivotal role in the early progression of DCM.[7,8] The excessive accumulation of lipids in the myocardium results in a disruption of energy substrate supply and utilization.[9] ATP can be derived from various energy substrates, including fatty acids, glucose, lactate, and ketone bodies. Fatty acids serve as the primary source of energy for the heart; however, the heart's capacity to synthesize fatty acids is limited and relies mainly on exogenous supply. In patients with type 2 diabetes, insulin resistance leads to a reduction in cardiac glucose utilization and oxidation capacity, thereby enhancing the acquisition and utilization of myocardial fatty acids.[7,10] Excessive oxidation of fatty acids generates toxic intermediates, such as palmitoyl-CoA and ceramides, which contribute to cardiac lipotoxicity in DCM. Cardiac lipotoxicity can induce an excessive production of reactive oxygen species (ROS), leading to oxidative damage to endogenous biomolecules including DNA, proteins, and unsaturated lipids. Ultimately, this process triggers apoptosis through both mitochondrial-dependent and independent pathways.[11]

Pigment epithelium-derived factor (PEDF) is a 50-kDa glycoprotein classified within the serine protease inhibitor superfamily.[12] PEDF is expressed in a diverse range of tissues and exhibits multifaceted biological activities, including anti-angiogenic, anti-apoptotic, antioxidant, and neuroprotective effects.[13–15] Recent studies have revealed that PEDF plays a crucial role in regulating cardiac energy metabolism, including glucose uptake and lipid metabolism.[16] On one hand, PEDF enhances glucose uptake in ischemic myocardium by up-regulating the expression of Glucose transporter type 4 (Glut4).[17] On the other hand, PEDF facilitates lipid metabolism through the regulation of CD36 expression, adipose triglyceride lipase (ATGL), and peroxisome proliferator-activated receptor(PPAR).[18–20] ATGL serves as the pivotal rate-limiting enzyme in triglyceride lipolysis, and myocardial overexpression of ATGL exhibits potential to mitigate diabetic cardiac lipotoxicity and ameliorate the progression of DCM.[21,22] Furthermore, numerous studies have demonstrated the protective effects of PEDF in cardiovascular diseases, such as ischemic heart disease[23,24] and atherosclerosis.[25] However, further investigation is required to determine whether PEDF can prevent DCM through regulation of cardiac energy metabolism.

The db/db mice, a well-established model of type 2 diabetes characterized by obesity, insulin resistance, hyperglycemia, hyperlipidemia, and concurrent cardiomyopathy, have been extensively utilized for the construction of a diabetic cardiomyopathy model.[26] In this study, we utilized AAV-PEDF tail vein injection to investigate the in vivo impact of PEDF on DCM. Furthermore, we validated these findings by transfecting H9c2 cells with PEDF plasmid with exposure to high glucose (HG) and palmitic acid (PA) treatment. Our study comprehensively examined the influence of PEDF on cardiac remodeling, cardiac function, cardiac lipotoxicity, energy metabolism, ROS, and apoptosis in db/db mice. Additionally, we further confirmed the crucial role of PEDF in modulating cardiac lipotoxicity, energy metabolism, ROS production, and apoptosis using a H9c2 cell model of DCM. Therefore, our study offers promising strategies for preventing DCM among individuals with diabetes in the future.

Materials and Methods

Construction of Adeno-Associated Virus Vector and Plasmid

The recombinant adeno-associated virus 9 (AAV9), which encodes either the mouse full-length PEDF gene (AAV9-PEDF, PubMed No. NM-011340) or green fluorescent protein (AAV9-GFP), was constructed and amplified. After confirming the sequence, the recombinant adeno-associated virus was purified (Genechem, Shanghai, China).

The full-length rat PEDF gene (PubMed No. NM-177927.2) was constructed into the pcDNA3.1-CMV-MCS-3flag-EF1-ZsGreen-T2A-Puro expression vector. The empty vector was used as a control plasmid. After confirming the sequence, the PEDF overexpression and control plasmids were extracted from bacteria solution (Hanbio, Shanghai, China) and transfected into the H9c2 cells using Lipo8000™ (C0533, Beyotime, China) following the manufacturer's instructions.

Animals

Seven-week-old male db/db and db/m mice were purchased from Rat Noble Biotechnology Co. Ltd (Beijing, China). Animal use protocols conform to the Guide for the Care and Use of Laboratory Animals published by the US National

Institutes of Health (the Eighth Edition, National Research Council 2011) and have been approved by the Animal Ethics Committee of Renmin Hospital of Wuhan University (No.20211203). All animals were kept under standard laboratory animal conditions (12h light/12h dark, adequate food, water, and a constant room temperature of 26 °C). All mice were sacrificed under anesthesia with sodium pentobarbital (50mg/kg, i.p; Sigma) to minimize their suffering.

Animal Grouping and Food Intake, Body Weight and Fasting Blood Glucose Testing

After adaptive feeding for one week, experimental animals were randomly divided into four groups: 1) DB/M group (db/m mice + normal saline, n=6); 2) DB/DB group (db/db mice + normal saline, n=6); 3) GFP group (db/db mice + AAV9-GFP, n=6); 4) PEDF group (db/db mice + AAV9-PEDF, n=6). The mice in GFP group and PEDF group were injected with AAV9-GFP and AAV9-PEDF via tail vein at a viral dose of $1E\times10^{12}$ v.g per mouse. The efficiency of virus infection and the expression of PEDF in db/db mice were confirmed by WB analysis. The body weight and food intake were measured every week and fasting blood glucose was measured by the glucometer (Sinocare, China) every four weeks.

Echocardiography

At 24 weeks, transthoracic echocardiography was used to assess cardiac function of db/m and db/db mice by the Vevo 3100 high Resolution Imaging System (VisualSonics Inc., Canada). After being anesthetized with isoflurane (1.5–2%, INH)., the mice's chest was depilated, and then the animals were immobilized. Left ventricular end-diastolic dimension (LVIDd) and left ventricular end-systolic dimension (LVIDs) were measured by M-mode echocardiography. Pulsed wave Doppler was applied to measure peak early (E), late (A) diastolic filling velocities. Peak early diastolic (e') and late diastolic (a') mitral annular velocities was measured by Tissue Doppler mode. Then left ventricular ejection fraction (LVEF), left ventricular fractional shortening (LVFS), E/A ratio and e'/ a' ratio were calculated.

Serological Detection

After completion of the echocardiography assay, the mice were anesthetized using 1% sodium pentobarbital solution (50 mg/kg; i.p; Sigma). Blood samples from the eye were collected, centrifuged, and stored at −80°C. The serum in each group were tested for triglyceride (TG), total cholesterol (TC), high-density cholesterol (HDL-Ch), low-density lipoprotein (LDL-Ch) and blood glucose using a fully-automated biochemical analyzer (Siemens Full-automatic Biochemical Analyzer, Centaur 2400).

Histological Analysis

After collecting blood samples from the eye, the hearts of mice were excised, fixed in 4% paraformaldehyde for 24 hours, embedded in paraffin, and sectioned at a thickness of 3 μm for pathological staining. The sections were subjected to hematoxylin-eosin (HE) and Masson trichrome staining. For the Oil Red O (ORO) staining, the frozen heart Section (3μm thickness) or cells climbing were stained with ORO working solutions for 30 min, washed with 60% isopropanol and then rinsed with PBS at least three times. Representative histopathologic images were captured using light microscopy (×200 magnification for HE staining, interstitial fibrosis and ORO staining; ×400 magnification for perivascular fibrosis; Nikon, Japan). Six samples from each group were randomly selected for analysis. The degree of cardiac hypertrophy, fibrosis and ORO^{+} area was analysed by Image J software.

Enzyme-Linked Immunosorbent Assay (ELISA)

The cardiac samples were collected and stored at −80 °C. The cardiac TG concentrations were determined with a mouse TG ELISA kit (J&L Biological, Shanghai, China) and the measurement procedure was carried out according to the manufacturer's instructions.

PA Synthesis

For palmitate (PA) preparation, fatty acid free BSA was added in 1× PBS (fatty acid free BSA:PBS, 0.2g:1mL) and then directly centrifuged at 8000r for 20min. After fatty acid free BSA dissolved in 1× PBS, sodium palmitate (P9767, Sigma)

(sodium palmitate: fatty acid free BSA, 1:35) was added and the palmitate-BSA solution was incubated for 30min at 75°C to generate a final concentration of 20mM (stock palmitate solution). The stock solution of PA was then filtered and diluted to 250μM concentration in DMEM for the subsequent studies.[27]

Cell Culture and Treatment

H9c2 cardiomyocytes were obtained from Procell Life Science&Technology Co.Ltd. (Wuhan, China). The H9c2 cells were cultured in the DMEM (Gibco) containing 10% FBS (Gibco) and 1% penicillin/strepto-mycin (Gibco) in the 5% CO2 atmosphere at 37°C. The H9c2 cells in 6-well plates was divided into four groups: 1) Control group (DMEM); 2) HG + PA group (33 mm glucose + 250μM PA); 3) HG + PA + h-GFP group (33 mm glucose + 250μM PA +h-GFP); 4) HG + PA + h-PEDF group (33 mm glucose + 250μM PA +h-PEDF). According to the experimental design, the H9c2 cells were firstly plated at an appropriate density and were cultured for 24 h to achieve 40–50% confluence before plasmid transfection. H9c2 cells in HG + PA + h-GFP group and HG + PA + h-PEDF group was transfected with h-GFP and h-PEDF plasmid. After 24 h plasmid transfection, HG + PA solution was added into DMEM medium for 24 h and then H9c2 cells were collected for follow-up experiments.

ROS and TUNEL Staining

ROS and TUNEL staining were evaluated using the ROS Assay Kit (CA1420, Solarbio, China) and the TUNEL Assay Kit (C1089, Beyotime, China) according to the standard protocol. Specifically, H9c2 cells which cultured in 6-well plates were transfected with plasmid. For ROS, 20μL DHE red fluorescent dye was added to 1mL DMEM medium after plasmid transfection for 48h. The mixture was incubated for 35 min at 37°C in the dark and then washed with 1× PBS twice. For TUNEL staining, H9c2 cells was fixed using 4% paraformaldehyde for 30min after plasmid transfection for 48h. Then 100ul TUNEL test solution was added in 6-well plates and the mixture was incubated for 60 min at 37°C in the dark. After washing with PBS for 3 times, the cell nucleus was stained with 4',6-diamidino-2-phenyl-indole (DAPI). At last, representative images were captured by a fluorescence microscope (×100 magnification; Nikon, Japan) and six samples from each group randomly selected for analysis by Image J software.

WB Analysis

Western blot analysis was performed according to previously described methods.[28] Briefly, tissues from the ventricle were digested with RIPA buffer containing phenylmethylsulfonyl fluoride and phosphatase inhibitors A and B. Extracted protein samples were subjected to electrophoresis, transferred to polyvinylidene difluoride (PVDF) membranes (Millipore, Hong Kong, China) and blocked with 5% nonfat dry milk in Tris-buffered saline Tween (TBST). Then, the protein was incubated with the following primary antibodies overnight at 4°C: PEDF rabbit antibody (1:1000, Abcam, ab227295), collagen I rabbit antibody (1:500, Abcam, ab279711), collagen III rabbit antibody (1:1000, Abcam, ab184993), HO-1 rabbit antibody (1:1000, Abcam, ab189491), ATGL rabbit antibody (1:1000, Proteintech, 55190-1-AP), PPARα mouse antibody (1:1000, Proteintech, 66826-1-Ig), CPT1α mouse antibody (1:1000, Proteintech, 66039-1-Ig), Bax rabbit antibody (1:1000, Immunoway, YM8175), Bcl2 rabbit antibody (1:1000, Proteintech,26593-1-AP), Caspase3 rabbit antibody (1:1000, Proteintech, 82202-1-RR), C-caspase3 rabbit antibody (1:1000, Cell Signaling Technology, 9664), Nrf2 rabbit antibody (1:1000, Baijia, IPB6621), CD 36 rabbit antibody (1:1000, Baijia, IPB0697), Glut4 rabbit antibody (1:1000, Baijia, IPB3253), and β-actin mouse antibody (1:3000, Proteintech, 66009-1-Ig). After washing with TBST three times, the membranes were incubated with goat anti-rabbit or goat anti-mouse secondary antibodies (1:10000, Aspen), and the protein bands were visualized by an enhanced chemiluminescence detection kit (Biosharp). The protein expression levels were quantified using Image J software and normalized to the β-actin protein.

Statistical Analysis

Statistical analysis was performed using GraphPad Prism 9.0 software. All data are expressed as the mean ± standard deviation (SD). One-way ANOVA followed by the Bonferroni-Dunn test was used for multiple comparisons of normally distributed data. A value of $P<0.05$ was considered statistically significant.

Results

PEDF Reverses Cardiac Remodeling in Db/Db Mice with Diabetic Cardiomyopathy

In this study, we initially assessed PEDF expression levels and the efficiency of viral infection in db/db mice. As illustrated in Figure 1A and B, compared with the DB/M group, PEDF expression was notably reduced in both the DB/DB and GFP groups, while it was significantly elevated in the PEDF group. The db/db mouse is a well-established model for type 2 diabetes,

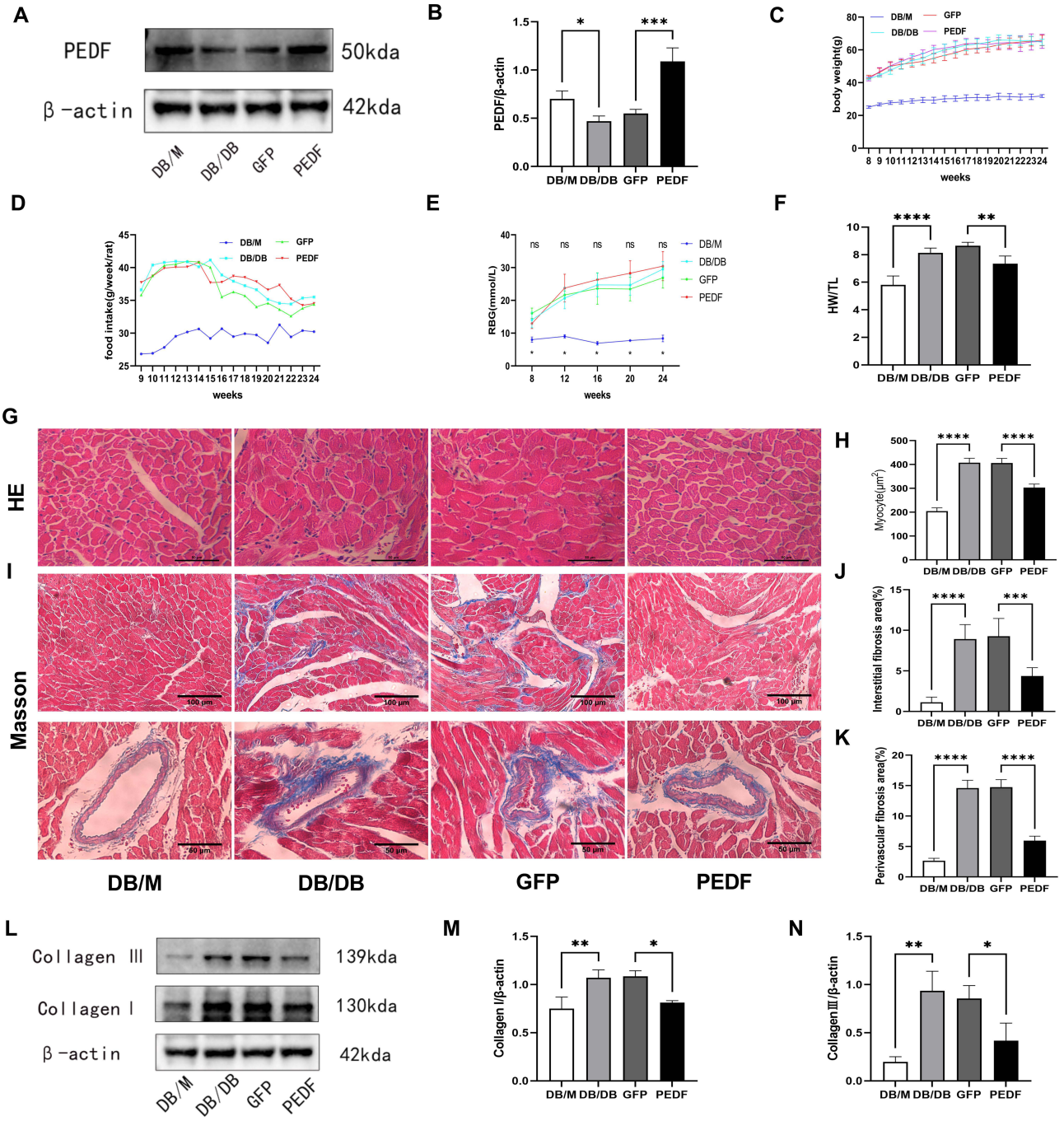

Figure 1 PEDF reverses cardiac remodeling in db/db mice with diabetic cardiomyopathy. (**A**)The representative Western blot images of PEDF, (**B**) Quantification of PEDF (n=3). The body weight(**C**), food intake(**D**) and blood glucose(**E**) were monitored at various time points. (**F**) The ratio of HW/TL (n=6). (**G** and **H**) Representative HE staining images and the relevant statistical graph (n=6). Bar = 50μm. (**I-K**) Representative Masson's trichrome staining images (up, interstitial fibrosis, bar = 100μm; down, perivascular fibrosis, bar = 50μm) and the relevant statistical graph (n=6). (**L**)The representative Western blot images of Collagen I and Collagen III,(**M**) Quantification of Collagen I (n=3), (**N**)Quantification of Collagen III (n=3). Data are expressed as mean ± SD. ****P<0.0001; ***P<0.001; **P<0.01; *P<0.05.

Abbreviations: ns, no significance; HW, heart weight; TL, tibial length.

https://doi.org/10.2147/DMSO.S482346

characterized by markedly increased food intake, hyperinsulinemia, hyperglycemia, hyperlipidemia, and obesity. In this study, we observed that the body weight, food intake, and fasting blood glucose levels of db/db mice were significantly higher compared to those of db/m mice. However, PEDF did not exert a significant influence on these parameters (Figure 1C–E). Cardiac hypertrophy and fibrosis are the primary characteristics of DCM. The heart weight to tibia length ratio (HW/TL), an indicator of cardiac hypertrophy, is significantly higher in the DB/DB group compared to the DB/M group. However, the HW/TL ratio in the PEDF group is notably lower than that in the GFP group (Figure 1F). Meanwhile, compared to the DB/M group, HE staining revealed significant cardiomyocyte hypertrophy in both the DB/DB and GFP group. This hypertrophy was notably reversed in the PEDF group (Figure 1G and H). Masson staining revealed that cardiac interstitial and perivascular fibrosis in the DB/DB and GFP groups were significantly higher compared to the DB/M group (Figure 1I–K). Additionally, the expression of collagen I and collagen III was markedly elevated in the DB/DB and GFP groups relative to the DB/M group (Figure 1L–N). However, overexpression of PEDF was found to mitigate cardiac interstitial and perivascular fibrosis, as well as the expression of collagen I and collagen III (Figure 1I–N). These data indicated that db/db mice can develop into DCM and PEDF can partly reverse cardiac remodeling of db/db mice at 24 weeks.

PEDF Ameliorates Deterioration of Cardiac Diastolic Function in Db/Db Mice

The presence of cardiac dysfunction in DCM prompted us to investigate the potential of PEDF in mitigating both systolic and diastolic dysfunction in db/db mice. Representative echocardiographic images were depicted as Figure 2A–C. Among the echocardiographic parameters, we observed that LVEF, EF, LVEDd, and LVEDs did not exhibit a reduction in the DB/DB and GFP groups compared to the DB/M group. Additionally, PEDF had no impact on improving systolic function (Figure 2D–G). However, diastolic dysfunction parameters such as E/A ratio and e'/a' ratio were reduced in DB/DB and GFP group compared with DB/M group and PEDF can improve these adverse effects (Figure 2H and I). These results demonstrated that PEDF has the potential to ameliorate diastolic dysfunction in db/db mice with DCM at 24 weeks.

PEDF Alleviates Cardiac Lipotoxicity and Regulates Cardiac Energy Metabolism in Db/Db Mice

The formation of DCM involves cardiac lipotoxicity and early alterations in cardiac energy metabolism. Based on the findings presented in Figure 3, we observed the impact of PEDF on cardiac lipotoxicity and energy metabolism. As depicted in Figures 3A–C, there is a higher deposition of cardiac neutral fats, such as triglycerides (TG), in the DB/DB and GFP groups compared to the DB/M group. However, PEDF administration can mitigate this excessive accumulation of neutral fats. Furthermore, the DB/DB group exhibited elevated serum triglycerides (TG), glucose (Glu), total cholesterol (TC), and decreased high-density lipoprotein cholesterol (HDL-Ch) levels compared to the DB/M group. However, db/db mice treated with AAV9-PEDF demonstrated a reduction in serum TG levels without affecting HDL-Ch, TC, or Glu (Figure 3D–G). The low-density lipoprotein cholesterol (LDL-Ch) levels showed no significant variation among the four groups (Figure 3H). To further explore the molecular mechanisms underlying the protective action of PEDF for cardiac lipotoxicity and energy metabolism in db/db mice, we evaluated the expression levels of ATGL, PPARα, CPT1α, CD36, and Glut4 which are closely associated with cardiac energy metabolism. The expression of PPARα, CPT1α, and CD36 was upregulated in the DB/DB and GFP group compared to the DB/M group, as shown in Figure 3I–N. However, PEDF supplementation significantly suppressed the expression of these proteins. Conversely, the expression of ATGL and Glut4 was downregulated in the DB/DB and GFP group compared to the DB/M group; however, PEDF supplementation notably promoted their expression (Figure 3I–N). These findings suggest that PEDF can effectively alleviate cardiac lipotoxicity and regulate cardiac energy metabolism in db/db mice.

PEDF Reduces ROS Production and Apoptosis in the Myocardium of Db/Db Mice

Cardiac lipotoxicity, which is markedly elevated in DCM, can lead to excessive ROS production and apoptosis. WB analysis demonstrated that the expression levels of heme oxygenase-1 (HO-1) and nuclear factor erythroid 2-related factor 2 (Nrf2) were lower in the DB/DB and GFP groups compared to the DB/M group (Figure 4A–C). Additionally, the DB/DB and GFP groups exhibited increased expression of Bax and cleaved caspase-3, along with decreased Bcl2

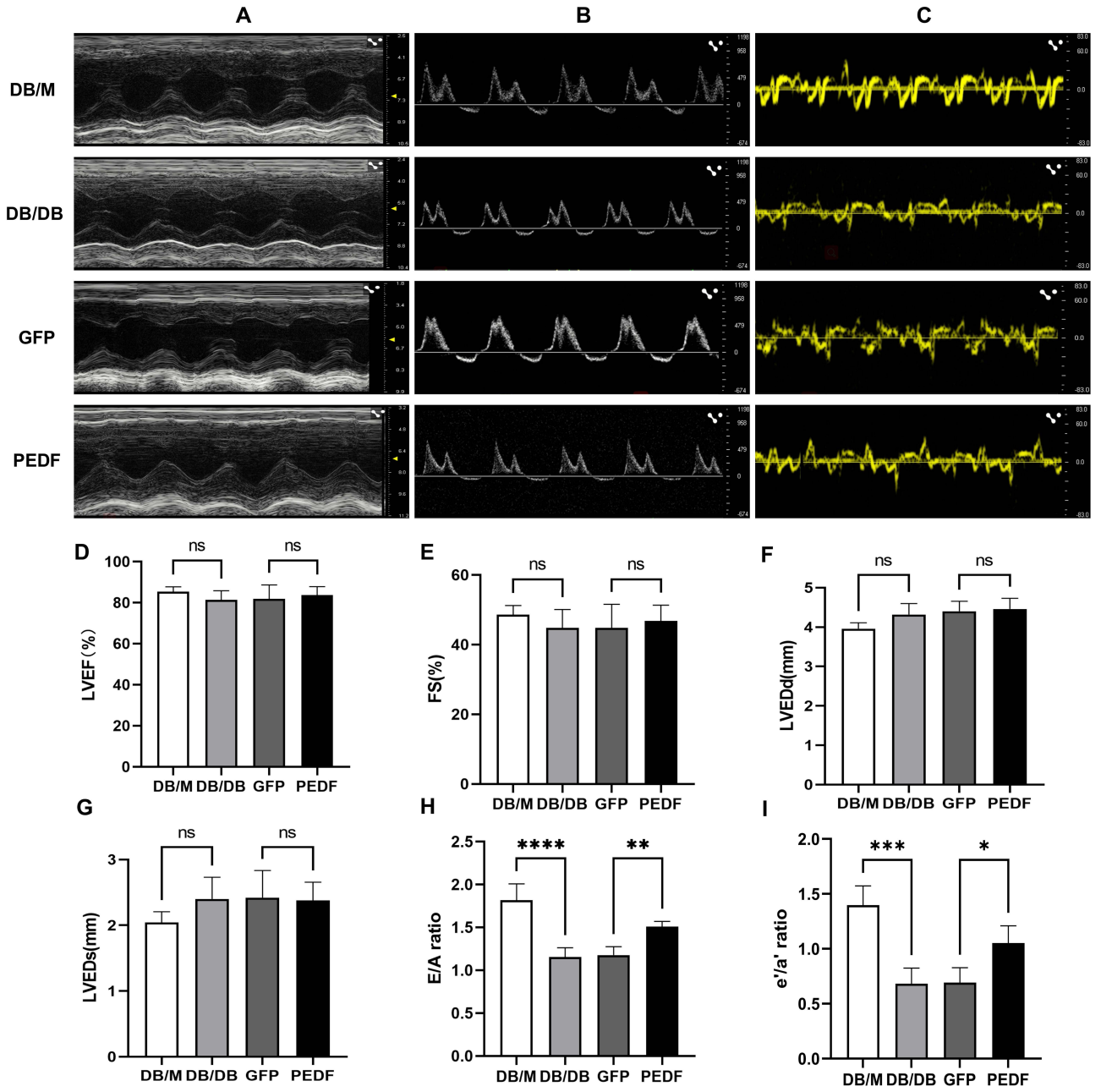

Figure 2 PEDF ameliorates deterioration of cardiac diastolic function in db/db mice. (**A**) Typical images of M-mode transthoracic echocardiography, (**D**)LVEF, (**E**)FS, (**F**) LVEDd and (**G**)LVEDs (n=6). (**B**) Representative images of pulsed-wave tissue Doppler transthoracic echocardiography, (**H**) mitral E/A ratio (n=6). (**C**) Representative images of tissue Doppler transthoracic echocardiography, (**I**) e'/a' ratio (n=6). Data are expressed as mean ± SD. ****P<0.0001; ***P<0.001; **P<0.01; *P<0.05; ns, no significance.

Abbreviations: LVEF, left ventricular ejection fraction; FS, fractional shortening; LVIDd, left ventricular end-diastolic diameter; LVIDs, left ventricular end-systolic diameter; E, early maximal ventricular filling velocity; A, atrial maximal ventricular filling velocity; e', peak early diastolic mitral annular velocity; a', late diastolic mitral annular velocity.

expression, relative to the DB/M group (Figure 4D–G). However, PEDF partly mitigated these protein alterations in db/db mice. These results indicated that PEDF can reduce ROS production and apoptosis of db/db mouse myocardium.

PEDF Reduces Lipid toxicity and Regulates Energy Metabolism in H9c2 Cells Treated with HG and PA

Under the conditions of high glucose and palmitic acid (HG and PA), the PEDF expression in H9c2 cells was significantly reduced. However, transfection with the PEDF plasmid markedly increased PEDF expression (Figure 5C and D). Compared to

https://doi.org/10.2147/DMSO.S482346

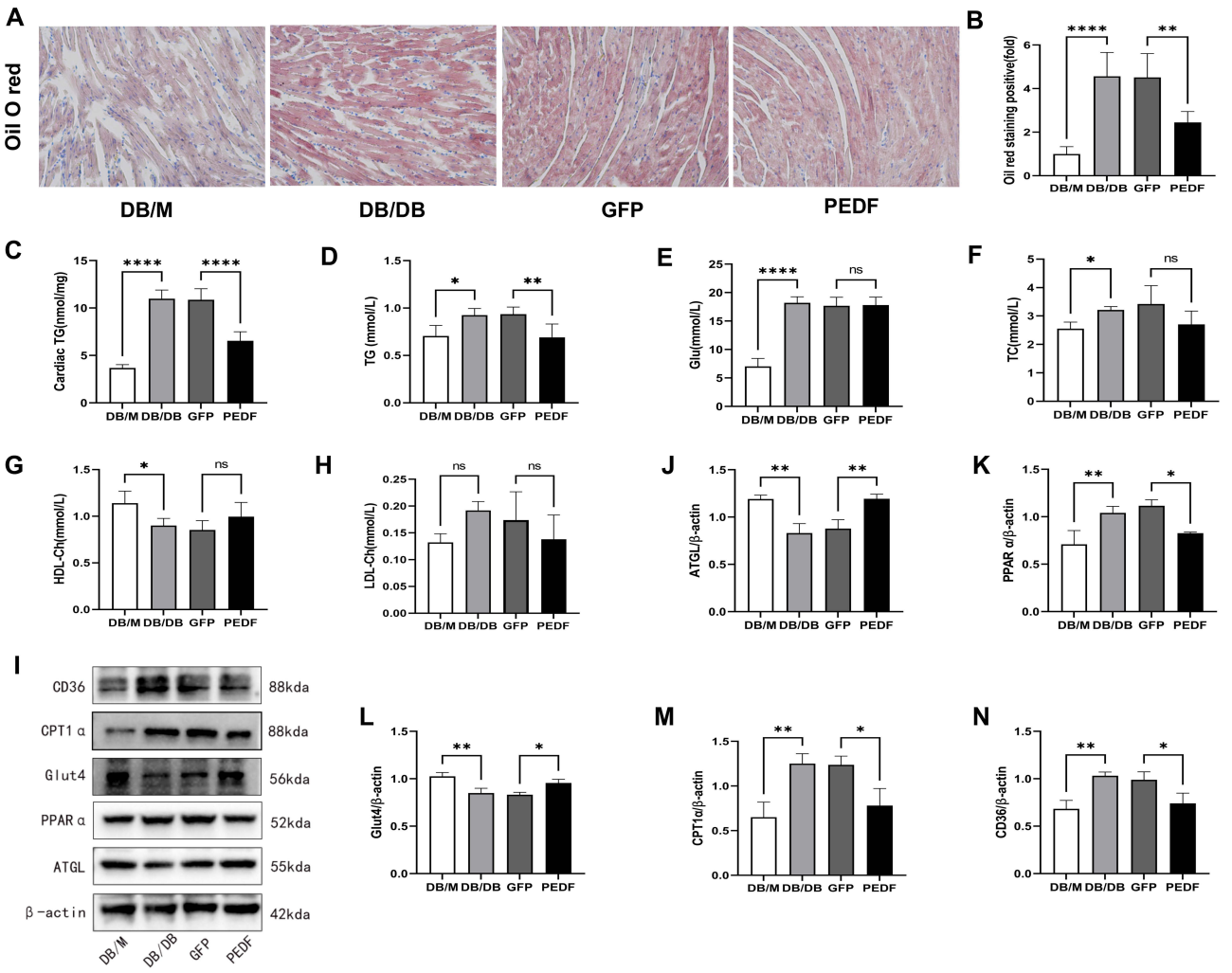

Figure 3 PEDF alleviates cardiac lipotoxicity and regulates cardiac energy metabolism in db/db mice. (**A** and **B**) Representative Oil O red staining images (×200) and the relevant statistical graph (n=6). (**C**) The TG concentrations of cardiac tissue (n=6). The TG(**D**), Glu(**E**), TC(**F**), HDL-Ch(**G**) and LDL-Ch(**H**) concentrations in serum were detected (n=6). (**I**)The representative Western blot images of ATGL, PPARα, Glut4, CPT1α and CD36, (**J-N**) Quantification of ATGL, PPARα, Glut4, CPT1αand CD36 (n=3). Data are expressed as mean ± SD. ****P<0.0001; **P<0.01; *P<0.05.

Abbreviations: ns, no significance; TG, triacylglycerol; Glu, glucose; LDL-Ch, low density lipoprotein cholesterin; HDL-Ch, high density lipoprotein cholesterin; TC, total cholesterin; ATGL, adipose triglyceride lipase; PPARα, peroxisome proliferator-activated receptor alpha; Glut4, glucose transporter type 4; CPT1α, carnitine palmitoyltransferase I alpha; CD36, scavenger receptor B2.

the control group, neutral fats including TG were increased in H9c2 cells treated with HG and PA. Moreover, PEDF can mitigate lipid accumulation in H9c2 cells (Figure 5A and B). To further investigate the effect of PEDF on energy metabolism in H9c2 cells treated with HG and PA, we detected the level of proteins that are related to glucose and lipid metabolism. As shown in Figure 5E–J, increased expression of PPAR α, CPT1α, and CD36, along with decreased expression of ATGL and Glut4, was observed in H9c2 cells treated with HG and PA compared to the control group. However, transfection with the PEDF plasmid significantly mitigated these alterations in H9c2 cells exposed to HG and PA. These findings suggested that PEDF is capable of mitigating lipid accumulation and modulating energy metabolism in H9c2 cells exposed to HG and PA.

PEDF Reduces ROS and Apoptosis in H9c2 Cells Exposed to HG and PA

As illustrated in Figure 6A–D, compared to the control group, the levels of ROS and apoptosis were elevated in H9c2 cells treated with HG and PA, but transfection with PEDF plasmid mitigated ROS generation and apoptosis. The results of WB analysis revealed that the expression levels of HO-1 and Nrf2 in H9c2 cells exposed to HG and PA were significantly lower compared to the control group. However, transfection with the PEDF plasmid markedly enhanced the

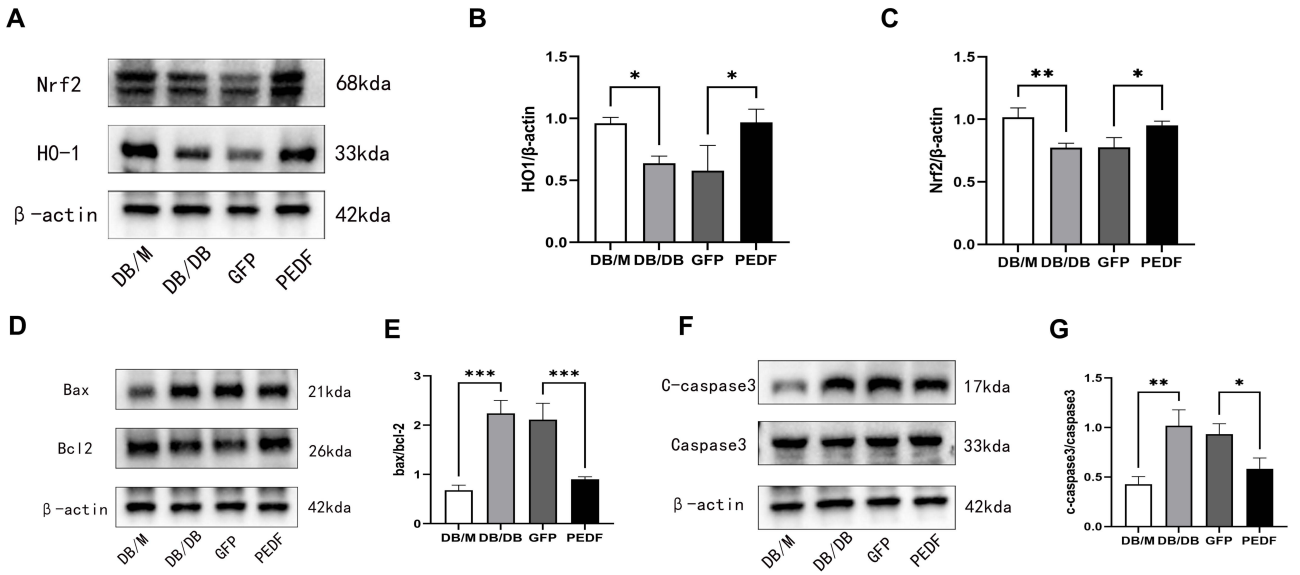

Figure 4 PEDF reduces ROS production and apoptosis in the myocardium of db/db mice. (**A**)The representative Western blot images of HO-1 and Nrf2, (**B** and **C**) Quantification of HO-1 and Nrf2 (n=3). (**D**) The representative Western blot images of Bax and Bcl2, (**E**) Quantification of Bax/Bcl2 (n=3). (**F**) The representative Western blot images of C-caspase3 and Caspase3, (**G**) Quantification of C-caspase3/Caspase3 (n=3). Data are expressed as mean ± SD. ***P<0.001; **P<0.01; *P<0.05. ROS, reactive oxygen species.

Abbreviations: HO-1, heme oxygenase 1; Nrf2, nuclear factor erythroid 2-related factor 2; Bcl2, B-cell lymphoma-2; Bax, Bcl2-associated X protein; Caspase3, cysteine-requiring aspartate protease 3; C-caspase3, cleaved cysteine-requiring aspartate protease 3.

expression of these proteins (Figure 6E–G). Meanwhile, an increase in Bax and C-caspase3 expression and a reduction in Bcl2 expression were observed in H9c2 cells treated with HG and PA compared to the control group, but PEDF plasmid transfection attenuated these changes in H9c2 cells exposed to HG and PA (Figure 4H–K). These results indicated that PEDF can reduce ROS and apoptosis in H9c2 cells treated with HG and PA.

Discussion

In the present study, we have demonstrated that PEDF expression is significantly downregulated in the hearts of db/db mice with DCM. Our findings reveal that PEDF overexpression alleviates cardiac hypertrophy, fibrosis, diastolic dysfunction, oxidative stress, and apoptosis induced by glucolipotoxicity through the modulation of energy metabolism. These results provide compelling evidence that PEDF plays a critical role in the pathogenesis of cardiac hypertrophy, fibrosis, and early metabolic alterations associated with DCM, suggesting that PEDF may represent a promising therapeutic target for the early prevention and intervention of DCM.

Approximately 45% of patients with heart failure with preserved ejection fraction (HFpEF) have diabetes mellitus and prolonged hyperglycemia can lead to diastolic dysfunction.[29] The db/db mouse is a typical type 2 diabetes model which showed features of diastolic dysfunction such as decreased E/A ratio. Apart from cardiac dysfunction, the other features of DCM include cardiomyocyte hypertrophy and myocardial fibrosis.[30] Similar to these findings, we found that db/db mice exhibited cardiomyocyte hypertrophy, cardiac interstitial and perivascular fibrosis and deteriorated diastolic function at 24 weeks. Meanwhile, PA was utilized to establish an in vitro cell model that mimics the excessive accumulation of cellular lipids and fatty acid oxidation in the pathological state of DCM.[31] Therefore, it is reasonable to use db/db mice and PA to construct in vivo and in vitro model of DCM in this study.

Typically, 60–70% of the heart's energy supply derived from free fatty acids (FFAs).[32] For metabolic syndrome, obesity, and diabetes, the excessive accumulation of FFAs in non-dipose tissues can result in impaired glucose and lipid metabolism, leading to lipotoxicity and insulin resistance.[33,34] DCM can induce an imbalance between the uptake and utilization of FFAs in cardiomyocytes, resulting in the excessive FFAs uptake and oxidation in the heart, which subsequently leads to myocardial cell damage.[35] Cardiac lipotoxicity, characterized by elevated myocardial triglyceride content, palmitoyl-CoA, and ceramide levels, is primarily caused by excessive FFA oxidation and plays a crucial role in the onset and progression of DCM. The influx

https://doi.org/10.2147/DMSO.S482346

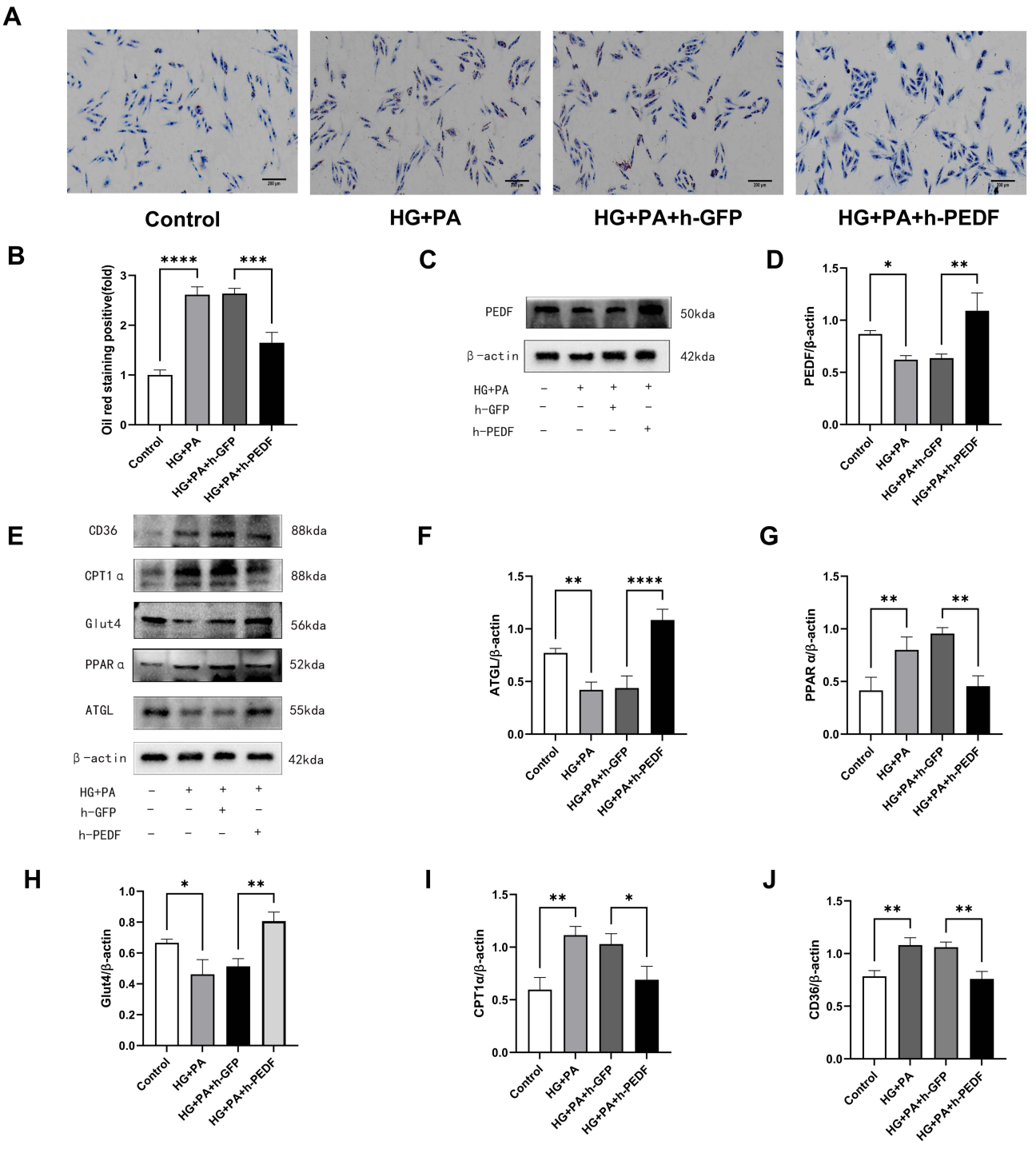

Figure 5 PEDF reduces lipid toxicity and regulates energy metabolism in H9c2 cells treated with HG and PA. (**A, B**) The representative Oil O red staining images of H9c2 cells and the relevant statistical graph (n=3). Bar = 200μm. (**C**)The representative Western blot images of PEDF, (**D**) Quantification of PEDF (n=3). (**E**) The representative Western blot images of ATGL, PPARα, Glut4, CPT1α and CD36, (**F-J**) Quantification of ATGL, PPARα, Glut4, CPT1αand CD36 (n=3). Data are expressed as mean ± SD. ****P<0.0001; ***P<0.001; **P<0.01; *P<0.05.

Abbreviations: HG, high glucose; PA, palmitate; ATGL, adipose triglyceride lipase; PPARα, peroxisome proliferator-activated receptor alpha; Glut4, glucose transporter type 4; CPT1α, carnitine palmitoyltransferase 1 alpha; CD36, scavenger receptor B2.

of circulating FFAs into cardiomyocytes is a critical step in lipotoxic myocardial injury. Studies have demonstrated that over 70% of the FFAs absorbed by cardiomyocytes are transported via protein-mediated active transport, primarily involving Fatty Acid Binding Protein 3(FABP3), CD36 and Fatty Acid Transport Protein 4(FATP4).[36] FABP3 and CD36 are the key

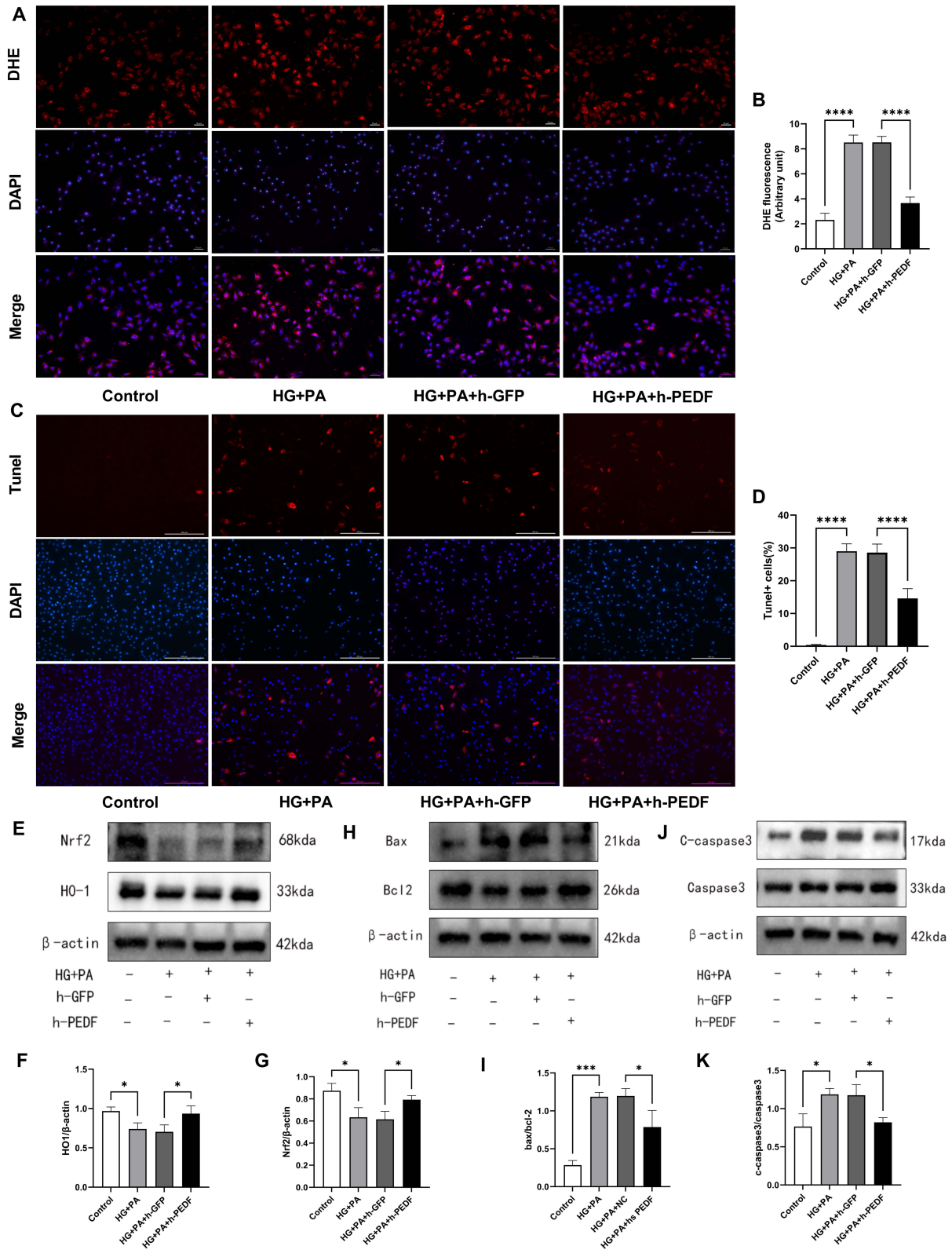

Figure 6 PEDF reduces ROS and apoptosis in H9c2 cells exposed to HG and PA. (**A** and **B**) Representative images and quantification of intracellular ROS production detected by DHE fluorescence (n=3). Bar = 50μm. (**C** and **D**) Representative images and quantification of Tunel staining (n=3). Bar = 200μm. (**E**)The representative Western blot images of HO-1 and Nrf2, (**F** and **G**) Quantification of HO-1 and Nrf2 (n=3). (**H**) The representative Western blot images of Bax and Bcl2, (**I**) Quantification of Bax/Bcl2 (n=3). (**J**) The representative Western blot images of C-caspase3 and Caspase3, (**K**) Quantification of C-caspase3/Caspase3 (n=3). Data are expressed as mean ± SD.****P<0.0001; ***P<0.001; *P<0.05.

Abbreviations: ROS, reactive oxygen species; HG, high glucose; PA, palmitate; DHE, Dihydroethidium; HO-1, heme oxygenase 1; Nrf2, nuclear factor erythroid 2-related factor 2; Bcl2, B-cell lymphoma-2; Bax, Bcl2-associated X protein; Caspase3, cysteine-requiring aspartate protease 3; C-caspase3, cleaved cysteine-requiring aspartate protease 3.

https://doi.org/10.2147/DMSO.S482346

transporters.[37] After delivery to cardiomyocytes, FFAs must enter the mitochondria for oxidation to produce ATP. During this process, CPT1α plays a crucial role in regulating the intracellular transport of FFAs.[38] Furthermore, PPARα is a ligand-activated transcription factor involved in the uptake and oxidation of FFAs.[39] Enhanced PPARα expression and activity can activate specific target genes, such as FABP3, CD36, FATP4, and CPT-1α, thereby augmenting the FFAs uptake and oxidation.[40] In our study, we observed PPARα, CPT-1α and CD36, which are involved in FFA uptake and oxidation, were upregulated in db/db mice. Treatment with PEDF significantly reversed these elevated protein expression changes. This indicates that in type 2 diabetes, the increased fatty acid uptake by cardiomyocytes is accompanied by enhanced fatty acid oxidation. Although this mechanism can transiently supply the myocardium with limited energy, it concurrently exacerbates myocardial oxidative stress and lipid toxicity. Following PEDF intervention, fatty acid uptake and oxidation in the diabetic myocardium were diminished, thereby mitigating lipid toxicity and oxidative stress. Correspondingly, increased myocardial FFAs uptake and oxidation are often accompanied by decreased glucose uptake in diabetes.[41] Given that Glut4 serves as one of the principal regulatory molecules in glucose transport, its downregulation is a critical indicator of diminished glucose uptake.[42] In this study, Glut4 expression was found to be downregulated in the hearts of db/db mice, whereas it was markedly upregulated in PEDF-overexpressing mice and cell models. This indicates that myocardial glucose uptake is diminished in diabetes due to insulin resistance, thereby affecting myocardial energy metabolism. Following PEDF intervention, the enhanced expression of Glut4 facilitates greater glucose uptake by the myocardium, thereby improving myocardial energy supply.

Myocardial lipotoxicity leads to extensive lipid droplet accumulation, and ATGL is the most crucial triglyceride hydrolase.[43] Previous studies have demonstrated that reduced cardiac function in both Akita and STZ diabetic models is closely associated with elevated cardiac TG deposition and downregulation of ATGL protein and mRNA levels.[44,45] Diabetes-induced diastolic dysfunction in ATGL KO mice was strongly associated with cardiac lipotoxicity. Conversely, ATGL gene overexpression was capable of reversing cardiac lipotoxicity in DCM,[22] which indicated that mice overexpressing ATGL exhibit significant resistance to diabetes-induced lipotoxicity. Meanwhile, TG content in myocardium is closely related to cardiac function in patients with diabetes and obesity.[46] TG depletion in cardiac apolipoprotein B overexpression mice and hormone-sensitive lipase (HSL) transgenic mice can reduce lipotoxicity and prevent pathological remodeling of the diabetic heart. However, some studies have shown that TG deposition is non-toxic to myocardium and can reduce FA oxidation through lipotoxic metabolic pathways.[47] In this study, we found that ATGL expression was significantly down-regulated in db/db mice and H9c2 cell models, and the overexpression of PEDF led to an upregulation of ATGL expression, resulting in the degradation of lipid droplets and subsequent production of fatty acids. It was expected that this increase in energy substrate would also enhance fatty acid oxidation, as indicated by elevated expression levels of PPARα and CPT-1α. However, repeated tests consistently showed reduced expression levels of PPARα and CPT-1α. Although we cannot provide evidence to explain why our findings contradict the observation that ATGL can activate PPARa ligands, a plausible explanation may be that cardiomyocyte fatty acids oxidation primarily relies on extracellular uptake of fatty acids rather than those produced through myocardial TG hydrolysis. These results suggested that upregulating ATGL while downregulating PPARα, CPT-1α, and CD36 can effectively mitigate cardiac lipid toxicity.

Oxidative stress represents a critical mechanism underlying tissue damage induced by lipotoxicity.[48] Under high-fat conditions, tissues take up large amounts of FFAs, resulting in excessive FFA oxidation. Consequently, oxygen consumption increases significantly, and substantial amounts of ROS are produced. In addition, the uptake and oxidation of FFAs can lead to the production of metabolic intermediates and ceramides, ultimately resulting in cardiomyocyte apoptosis via the mitochondrial pathway. Excessive FFA oxidation significantly increases myocardial oxygen consumption and ROS production, thereby inducing oxidative stress and subsequent myocardial injury. The Nrf2 pathway, which is closely associated with antioxidant responses, becomes activated in response to the onset of oxidative stress.[49] In the present study, we found that the protein expression levels of cardiac Nrf2 and its target genes HO-1 were significantly reduced in hearts of db/db mice. However, overexpression of PEDF was able to effectively promote the expression of both Nrf2 and HO-1. The role of apoptosis in the deterioration of cardiac function in db/db mice was also investigated. It was found that the expression levels of pro-apoptotic proteins Bax and C-caspase3 were significantly increased, while the expression of the anti-apoptotic protein Bcl2 was significantly reduced. However, PEDF overexpression could reverse

these changes. These findings indicate that PEDF overexpression attenuates ROS accumulation and apoptosis resulting from cardiac lipotoxicity.

The present study has several limitations. First, we did not investigate the effects of PEDF in non-obese type 2 diabetes mice, and cardiac energy metabolism differs significantly between obese and non-obese type 2 diabetes mellitus.[8] Second, while this study primarily focused on the effects of PEDF on cardiac energy metabolism, ROS, and apoptosis, we did not explore other potential roles of PEDF, such as mitochondrial dysfunction and autophagy in DCM. Third, the specific mechanisms by which PEDF regulates cardiac energy metabolism remain unclear and require further investigation.

Conclusion

PEDF alleviates ectopic fat deposition and fibrosis in DCM and improves diastolic function. This may be related to the fact that PEDF can improve myocardial energy metabolism, by reducing fatty acid intake and oxidation while increasing glucose uptake in the diabetic myocardium. Meanwhile, PEDF can inhibit oxidative stress and myocardial cell apoptosis. These mechanisms suggest that PEDF is a promising therapeutic target for DCM.

Myocardial ATP reserves are limited, yet the heart's continuous contraction necessitates a substantial and sustained energy supply. Consequently, the myocardium possesses the remarkable ability to generate large quantities of ATP continuously from a variety of energy substrates, including fatty acids, glucose, lactate, ketone bodies, and amino acids. Fatty acid and glucose are two important fuels of the heart, and their balanced utilization is an important guarantee to maintain the normal contraction of the heart. Given the evidence that PEDF plays a role in regulating energy metabolism, future research could integrate metabolomics to elucidate the specific mechanisms by which PEDF modulates energy metabolism in diabetic myocardium.

Funding

This research was supported by the National Natural Science Foundation of China (NO. 82100866) to Tuohua Mao.

Disclosure

The authors report no conflicts of interest in this work.

References

1. Wong ND, Sattar N. Cardiovascular risk in diabetes mellitus: epidemiology, assessment and prevention. *Nat Rev Cardiol*. 2023;20(10):685–695. doi:10.1038/s41569-023-00877-z
2. Dillmann WH. Diabetic cardiomyopathy. *Circ Res*. 2019;124(8):1160–1162. doi:10.1161/CIRCRESAHA.118.314665
3. van de Weijer T, Schrauwen-Hinderling VB, Schrauwen P. Lipotoxicity in type 2 diabetic cardiomyopathy. *Cardiovasc Res*. 2011;92(1):10–18. doi:10.1093/cvr/cvr212
4. Finck BN, Han X, Courtois M, et al. A critical role for PPARalpha-mediated lipotoxicity in the pathogenesis of diabetic cardiomyopathy: modulation by dietary fat content. *Proc Natl Acad Sci U S A*. 2003;100(3):1226–1231. doi:10.1073/pnas.0336724100
5. Feng Y, Xu W, Zhang W, Wang W, Liu T, Zhou X. LncRNA DCRF regulates cardiomyocyte autophagy by targeting miR-551b-5p in diabetic cardiomyopathy. *Theranostics*. 2019;9(15):4558–4566. doi:10.7150/thno.31052
6. Hu L, Ding M, Tang D, et al. Targeting mitochondrial dynamics by regulating Mfn2 for therapeutic intervention in diabetic cardiomyopathy. *Theranostics*. 2019;9(13):3687–3706. doi:10.7150/thno.33684
7. Rodrigues B, Cam MC, McNeill JH. Metabolic disturbances in diabetic cardiomyopathy. *Mol Cell Biochem*. 1998;180(1–2):53–57. doi:10.1023/A:1006882805197
8. Li X, Wu Y, Zhao J, et al. Distinct cardiac energy metabolism and oxidative stress adaptations between obese and non-obese type 2 diabetes mellitus. *Theranostics*. 2020;10(6):2675–2695. doi:10.7150/thno.40735
9. Fang ZY, Prins JB, Marwick TH. Diabetic cardiomyopathy: evidence, mechanisms, and therapeutic implications. *Endocr Rev*. 2004;25(4):543–567. doi:10.1210/er.2003-0012
10. Saddik M, Lopaschuk GD. Triacylglycerol turnover in isolated working hearts of acutely diabetic rats. *Can J Physiol Pharmacol*. 1994;72(10):1110–1119. doi:10.1139/y94-157
11. Sinha K, Das J, Pal PB, Sil PC. Oxidative stress: the mitochondria-dependent and mitochondria-independent pathways of apoptosis. *Arch Toxicol*. 2013;87(7):1157–1180. doi:10.1007/s00204-013-1034-4
12. Matsui T, Nishino Y, Ojima A, Maeda S, Tahara N, Yamagishi SI. Pigment epithelium-derived factor improves metabolic derangements and ameliorates dysregulation of adipocytokines in obese type 2 diabetic rats. *Am J Pathol*. 2014;184(4):1094–1103. doi:10.1016/j.ajpath.2013.12.032
13. Yamagishi SI, Matsui T. Anti-atherothrombogenic properties of PEDF. *Curr Mol Med*. 2010;10(3):284–291. doi:10.2174/156652410791065264
14. Wang X, Zhang Y, Lu P, et al. PEDF attenuates hypoxia-induced apoptosis and necrosis in H9c2 cells by inhibiting p53 mitochondrial translocation via PEDF-R. *Biochem Biophys Res Commun*. 2015;465(3):394–401. doi:10.1016/j.bbrc.2015.08.015
15. Lu P, Qi Y, Li X, et al. PEDF and 34-mer peptide inhibit cardiac microvascular endothelial cell ferroptosis via Nrf2/HO-1 signalling in myocardial ischemia-reperfusion injury. *J Cell Mol Med*. 2024;28(14):e18558. doi:10.1111/jcmm.18558

16. Kiss A, Podesser BK. Cardioprotection by PEDF: a novel form of GLUT4 membrane translocation to reduce myocardial ischemic injury. *Int J Cardiol*. 2019;288:119–120. doi:10.1016/j.ijcard.2019.04.045
17. Yuan Y, Liu X, Miao H, et al. PEDF increases GLUT4-mediated glucose uptake in rat ischemic myocardium via PI3K/AKT pathway in a PEDFR-dependent manner. *Int J Cardiol*. 2019;283:136–143. doi:10.1016/j.ijcard.2019.02.035
18. Zhang H, Sun T, Jiang X, et al. PEDF and PEDF-derived peptide 44mer stimulate cardiac triglyceride degradation via ATGL. *J Transl Med*. 2015;13(68):68. doi:10.1186/s12967-015-0432-1
19. Yang S, Luo T, Zhou H, et al. Rosiglitazone inhibits expression and secretion of PEDF in adipose tissue and liver of male SD rats via a PPAR-γ independent mechanism. *Endocrinology*. 2014;155(3):941–950. doi:10.1210/en.2013-1813
20. Huang KT, Hsu LW, Chen KD, Kung CP, Goto S, Chen CL. Decreased PEDF expression promotes adipogenic differentiation through the up-regulation of CD36. *Int J mol Sci*. 2018;19(12):3992. doi:10.3390/ijms19123992
21. Cui W, Sathyanarayan A, Lopresti M, Aghajan M, Chen C, Mashek DG. Lipophagy-derived fatty acids undergo extracellular efflux via lysosomal exocytosis. *Autophagy*. 2021;17(3):690–705. doi:10.1080/15548627.2020.1728097
22. Pulinilkunnil T, Kienesberger PC, Nagendran J, et al. Myocardial adipose triglyceride lipase overexpression protects diabetic mice from the development of lipotoxic cardiomyopathy. *Diabetes*. 2013;62(5):1464–1477. doi:10.2337/db12-0927
23. Kajikawa M, Maruhashi T, Iwamoto Y, et al. Circulating level of pigment epithelium-derived factor is associated with vascular function and structure: a cross-sectional study. *Int J Cardiol*. 2016;225:91–95. doi:10.1016/j.ijcard.2016.09.123
24. Rychli K, Kaun C, Hohensinner PJ, et al. The anti-angiogenic factor PEDF is present in the human heart and is regulated by anoxia in cardiac myocytes and fibroblasts. *J Cell Mol Med*. 2010;14(1–2):198–205. doi:10.1111/j.1582-4934.2009.00731.x
25. Baba H, Yonemitsu Y, Nakano T, et al. Cytoplasmic expression and extracellular deposition of an antiangiogenic factor, pigment epithelium-derived factor, in human atherosclerotic plaques. *Arterioscler Thromb Vasc Biol*. 2005;25(9):1938–1944. doi:10.1161/01.ATV.0000175759.78338.1e
26. Chen H, Charlat O, Tartaglia LA, et al. Evidence that the diabetes gene encodes the leptin receptor: identification of a mutation in the leptin receptor gene in db/db mice. *Cell*. 1996;84(3):491–495. doi:10.1016/S0092-8674(00)81294-5
27. Zhang B, Li X, Liu G, et al. Peroxiredomin-4 ameliorates lipotoxicity-induced oxidative stress and apoptosis in diabetic cardiomyopathy. *Biomed Pharmacother*. 2021;141(111780):111780. doi:10.1016/j.biopha.2021.111780
28. Wang D, Yin Y, Wang S, et al. FGF1(ΔHBS) prevents diabetic cardiomyopathy by maintaining mitochondrial homeostasis and reducing oxidative stress via AMPK/Nur77 suppression. *Signal Transduct Target Ther*. 2021;6(1):133. doi:10.1038/s41392-021-00542-2
29. McHugh K, DeVore AD, Wu J, et al. Heart failure with preserved ejection fraction and diabetes: JACC state-of-the-art review. *J Am Coll Cardiol*. 2019;73(5):602–611. doi:10.1016/j.jacc.2018.11.033
30. Belke DD, Larsen TS, Gibbs EM, Severson DL. Altered metabolism causes cardiac dysfunction in perfused hearts from diabetic (db/db) mice. *Am J Physiol Endocrinol Metab*. 2000;279(5):E1104–1113. doi:10.1152/ajpendo.2000.279.5.E1104
31. Lee E, Lee HS. Peroxidase expression is decreased by palmitate in cultured podocytes but increased in podocytes of advanced diabetic nephropathy. *J Cell Physiol*. 2018;233(12):9060–9069. doi:10.1002/jcp.26875
32. Neely JR, Morgan HE. Relationship between carbohydrate and lipid metabolism and the energy balance of heart muscle. *Annu Rev Physiol*. 1974;36:413–459. doi:10.1146/annurev.ph.36.030174.002213
33. Stefan N, Häring HU. Circulating fetuin-A and free fatty acids interact to predict insulin resistance in humans. *Nat Med*. 2013;19(4):394–395. doi:10.1038/nm.3116
34. Jia G, DeMarco VG, Sowers JR. Insulin resistance and hyperinsulinaemia in diabetic cardiomyopathy. *Nat Rev Endocrinol*. 2016;12(3):144–153. doi:10.1038/nrendo.2015.216
35. Kenny HC, Abel ED. Heart Failure in Type 2 Diabetes Mellitus. *Circ Res*. 2019;124(1):121–141. doi:10.1161/CIRCRESAHA.118.311371
36. Chabowski A, Górski J, Glatz JF, L JJP, Bonen A. Protein-mediated fatty acid uptake in the heart. *Curr Cardiol Rev*. 2008;4(1):12–21.
37. Carley AN, Kleinfeld AM. Fatty acid (FFA) transport in cardiomyocytes revealed by imaging unbound FFA is mediated by an FFA pump modulated by the CD36 protein. *J Biol Chem*. 2011;286(6):4589–4597. doi:10.1074/jbc.M110.182162
38. Schwenk RW, Luiken JJ, Bonen A, Glatz JF. Regulation of sarcolemmal glucose and fatty acid transporters in cardiac disease. *Cardiovasc Res*. 2008;79(2):249–258. doi:10.1093/cvr/cvn116
39. Lv J, Deng C, Jiang S, et al. Blossoming 20: the energetic regulator's birthday unveils its versatility in cardiac diseases. *Theranostics*. 2019;9(2):466–476. doi:10.7150/thno.29130
40. Liu F, Song R, Feng Y, et al. Upregulation of MG53 induces diabetic cardiomyopathy through transcriptional activation of peroxisome proliferation-activated receptor α. *Circulation*. 2015;131(9):795–804.
41. Boudina S, Abel ED. Diabetic cardiomyopathy revisited. *Circulation*. 2007;115(25):3213–3223. doi:10.1161/CIRCULATIONAHA.106.679597
42. Garvey WT, Hardin D, Juhaszova M, Dominguez JH. Effects of diabetes on myocardial glucose transport system in rats: implications for diabetic cardiomyopathy. *Am J Physiol Cell Physiol*. 1993;264(3 Pt 2):H837–844. doi:10.1152/ajpheart.1993.264.3.H837
43. Zechner R, Zimmermann R, Eichmann TO, et al. FAT SIGNALS--lipases and lipolysis in lipid metabolism and signaling. *Cell Metabolism*. 2012;15(3):279–291.
44. Basu R, Oudit GY, Wang X, et al. Type 1 diabetic cardiomyopathy in the akita (Ins2WT/C96Y) mouse model is characterized by lipotoxicity and diastolic dysfunction with preserved systolic function. *Am J Physiol Heart Circ Physiol*. 2009;297(6):H2096–2108. doi:10.1152/ajpheart.00452.2009
45. Finck BN, Lehman JJ, Leone TC, et al. The cardiac phenotype induced by PPARalpha overexpression mimics that caused by diabetes mellitus. *J Clin Invest*. 2002;109(1):121–130. doi:10.1172/JCI0214080
46. Hammer S, Snel M, Lamb HJ, et al. Prolonged caloric restriction in obese patients with type 2 diabetes mellitus decreases myocardial triglyceride content and improves myocardial function. *J Am Coll Cardiol*. 2008;52(12):1006–1012. doi:10.1016/j.jacc.2008.04.068
47. Listenberger LL, Han X, Lewis SE, Cases S, Farese R V ODS Jr, Schaffer JE. Triglyceride accumulation protects against fatty acid-induced lipotoxicity. *Proc Natl Acad Sci U S A*. 2003;100(6):3077–3082.
48. Bugger H, Abel ED. Molecular mechanisms of diabetic cardiomyopathy. *Diabetologia*. 2014;57(4):660–671.
49. Buendia I, Michalska P, Navarro E, Gameiro I, Egea J, León R. Nrf2-ARE pathway: an emerging target against oxidative stress and neuroinflammation in neurodegenerative diseases. *Pharmacol Ther*. 2016;157:84–104. doi:10.1016/j.pharmthera.2015.11.003